

# Cardiac Magnetic Resonance Imaging for the Investigation of Cardiovascular Disorders.

## Part 2: Emerging Applications

Ajit H. Goenka, MD  
Hui Wang, PhD  
Scott D. Flamm, MD, MBA

*Cardiac magnetic resonance imaging has emerged as a robust noninvasive technique for the investigation of cardiovascular disorders. The coming-of-age of cardiac magnetic resonance—and especially its widening span of applications—has generated both excitement and uncertainty in regard to its potential clinical use and its role vis-à-vis conventional imaging techniques. The purpose of this evidence-based review is to discuss some of these issues by highlighting the current (Part 1, previously published) and emerging (Part 2) applications of cardiac magnetic resonance. Familiarity with the versatile uses of cardiac magnetic resonance will facilitate its wider clinical acceptance for improving the management of patients with cardiovascular disorders. (Tex Heart Inst J 2014;41(2):135-43)*

**Key words:** Cardiomyopathies/diagnosis; fibrosis; gadolinium DTPA/diagnostic use; hypertrophy, left ventricular/diagnosis; magnetic resonance angiography; magnetic resonance imaging/standards; myocarditis/diagnosis; pericarditis, constrictive/diagnosis; sarcoidosis; stroke volume; ventricular dysfunction, left/diagnosis

**From:** Cardiovascular Imaging Laboratory, Imaging Institute, Cleveland Clinic; and Cardiovascular Medicine, Heart and Vascular Institute, Cleveland Clinic (Drs. Flamm and Goenka), Cleveland, Ohio 44195; and Philips Healthcare (Dr. Wang), Highland Heights, Ohio 44143

**Address for reprints:** Scott D. Flamm, MD, MBA, Cardiovascular Imaging Laboratory, J1-4, Imaging Institute, Cleveland Clinic, 9500 Euclid Ave., Cleveland, OH 44195

**E-mail:** flamms@ccf.org

© 2014 by the Texas Heart<sup>®</sup> Institute, Houston

**C**ardiac magnetic resonance imaging (CMR) is unique in its ability to provide comprehensive evaluation of cardiovascular disorders in a single session. Part 1 of this review highlighted the mainstream applications of CMR that are now routinely used for diagnosis, risk stratification, and case management.<sup>1</sup> In this section, we provide an overview of the principles and potential applications of emerging CMR techniques that seek to characterize the myocardial substrate in both health and disease. These techniques offer the ability to noninvasively delineate pathophysiologic processes in vivo and, therefore, to expand our understanding of cardiovascular disorders. We also present a synopsis of innovative applications of validated CMR techniques that have the potential to expand the usefulness of CMR as a clinically relevant, cost-effective tool for reliable investigation and accurate case management in a wide variety of clinical situations.

### T1 Mapping and Extracellular Volume Quantification

Detection of regional or replacement myocardial fibrosis on CMR arises from the visual evaluation of well-delineated areas of late gadolinium enhancement (LGE) on delayed-enhancement MR (DE-MR) imaging. As discussed in Part 1 of this review,<sup>1</sup> high contrast-to-noise ratio in DE-MR imaging is achieved by suppressing the signal from the normal, unaffected myocardium. However, in patients with diffuse interstitial fibrosis, defining the unaffected myocardium can be difficult, which limits the usefulness of DE-MR imaging for detecting diffuse myocardial processes and for quantifying the extent of extracellular matrix (ECM) expansion. Therefore, direct quantification of longitudinal relaxation time of tissue (T1) has been proposed as a novel alternative imaging biomarker of myocardial fibrosis.

Depending on the composition of the tissue, T1 relaxation times vary across tissue types. Deviation from established ranges can therefore be used to quantify the effects of pathologic processes.<sup>2</sup> The generation of parametric maps that encode T1 value in each pixel of an image is called T1 mapping (Fig. 1).

Not only does T1 mapping provide quantitative estimation of diffuse myocardial disease processes and extracellular volume (ECV), but it has the advantage (when compared with DE-MR imaging) of circumventing the influences of windowing, of variations in signal enhancement, and of variability of observer input in characterizing the diseased myocardium.<sup>3</sup> Recent robust developments in acquisition and post-processing techniques have given T1 mapping significant traction. Key acquisition

sequences include the Modified Lock-Lock Inversion Recovery (MOLLI)<sup>4</sup> sequence and its variations, such as shortened MOLLI (ShMOLLI).<sup>2</sup> The 2 principal CMR measurements obtained by using this method are native T1 and ECV.

**Native T1.** Native (precontrast or noncontrast) T1 mapping elicits tissue differences without the use of a gadolinium-based contrast agent (GBCA). This feature is particularly appealing for application to patients with significant renal insufficiency (in whom GBCAs have been associated with nephrogenic systemic fibrosis<sup>5</sup>) and application to pregnant patients (in whom GBCAs are contraindicated). Native T1 measures the composite signal from both the interstitium and the myocytes.<sup>6</sup> When compared with measurements of ECV and LGE, measurement of native T1 has the advantage of detecting the deposition of pathologically important substances such as iron, fat, and other T1-altering substances.<sup>7</sup> Native T1 mapping has shown high accuracy in detecting myocardial edema and has been proposed

as a complementary technique to T2-weighted (T2W) imaging.<sup>8</sup> This technique is, however, quite sensitive to the methods of acquisition and postprocessing.

**Extracellular Volume.** Extracellular volume measures the space occupied by the ECM, which is a surrogate measure of ECM itself and uses GBCA as an extracellular space marker. The bright signal generated on T1-weighted (T1W) images—due to the T1-shortening effect of GBCAs—points to the ECM. Consequently, it can be said that ECV attempts to divide the myocardium into its cellular and interstitial components, with estimates expressed as volume fractions.<sup>7</sup> Extracellular volume maps are generated by quantifying the native and postcontrast T1 values on co-registered images while adjusting for the hematocrit,<sup>9</sup> in order to account for the effects of changes in body composition, renal function, and hematocrit due to the underlying disease process.

The ability to noninvasively quantify ECM alterations is an important advance in CMR. Extracellular volume directly quantifies the relative expansion of ECM imposed by collagen deposition. However, ECM expansion can also be caused by myocardial edema or infiltrative disorders such as amyloidosis. Given the pathophysiologic significance of myocardial ECM, ECV measures might be of prognostic significance equivalent to left ventricular (LV) ejection fraction.<sup>7,9,10</sup> Extracellular matrix is a modifiable target in several disease processes—so T1 mapping might find wide applicability in disease characterization, monitoring, outcome prediction, and therapeutics.<sup>11</sup>

Initial clinical results have been promising. Both pre-contrast and postcontrast T1 values have provided high diagnostic accuracy in differentiating between normal and diffusely diseased myocardium in patients with hypertrophic obstructive cardiomyopathy (HOCM) and nonischemic cardiomyopathy (NICM), with native T1 values showing the highest accuracy.<sup>12</sup> Quantitative T1 measurement using equilibrium contrast (EQ)-CMR has also shown strong correlation to histology for quantification of diffuse myocardial fibrosis in patients with aortic stenosis or HOCM.<sup>11</sup> Moreover, T1 mapping has been validated for the evaluation of interstitial fibrosis in patients with clinically evident cardiomyopathy, including those without focal LGE.<sup>13</sup> These techniques have also been used to gain additional insights into the pathophysiologic role of ECM. For instance, a study using T1 mapping and other CMR measurements suggested that ECM expansion in remote myocardium might be linked to adverse remodeling after acute myocardial infarction (MI).<sup>14</sup> An association between ECV, short-term death, and other adverse clinical outcomes also has been recently shown<sup>9</sup>; this association appears to be stronger with ECV than with LGE.<sup>7</sup> On the basis of this association, the use of ECV as a biomarker for risk stratification has been proposed.

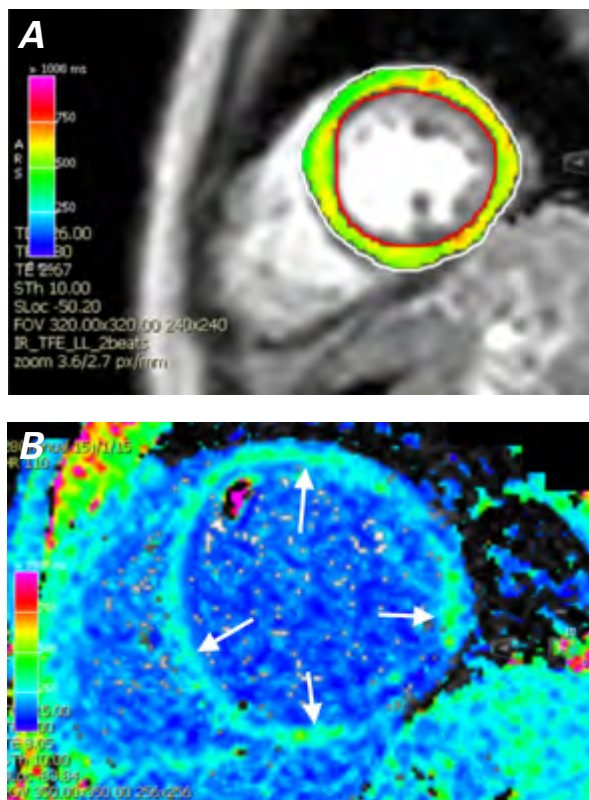


**Fig. 1 A)** Parametric overlay of a T1 map on a short-axis slice of left ventricle (yellow ring) in a healthy volunteer. The color scale of yellow in this image corresponds to a mean T1 value of 563 ms. **B)** A 43-year-old woman with dilated nonischemic cardiomyopathy has diffusely abnormal T1 values throughout the left ventricular myocardium (arrows). The T1 values of the myocardium have a mean value of 174 ms, which corresponds to the green-blue portion of the parametric color scale (seen on the left border of the image).

These promising results notwithstanding, the integration of these techniques into routine clinical MR scanning protocols is challenging. All of the factors that influence the precision of measured native T1 values have not been completely characterized, and broad scientific consensus about the protocols for image acquisition, postprocessing, and interpretation has not yet been achieved. Nonetheless, T1 mapping represents an innovative addition to other CMR measures of tissue characterization. Multicenter trials must investigate and validate the effect of these techniques on the management of cardiovascular disorders.

## T2 Mapping

Cardiac magnetic resonance is the only noninvasive imaging technique that can detect myocardial edema. This has traditionally been performed with water-sensitive T2W imaging, on the principle that prolongation of T2-relaxation time due to the increased mobility of water protons in edematous myocardium results in increased T2 signal intensity. Myocardial edema is believed to be a fundamental response to ischemia reperfusion injury. Therefore, an interesting application of T2W imaging has been in the demarcation of the area at risk associated with acute MI.<sup>15,16</sup> The area at risk during an acute coronary event is the salvageable myocardium (hypoperfused but noninfarcted), the salvation of which can determine the therapeutic efficacy of reperfusion therapy.<sup>17</sup> The clinical significance of detecting the area at risk cannot be overemphasized. However, the clinical interpretation of T2W imaging is subjective and can be ambiguous because of low signal-to-noise ratio (SNR), variability in signal intensity from the surface coil, high T2 signal from slow stagnant blood near the blood pool–endocardial interface, and motion artifacts. To overcome some of these limitations, quantitative T2

mapping has recently been introduced for the objective evaluation of myocardial T2 relaxation time (Fig. 2).

Quantitative approaches are less prone to artifacts, are independent of the heart rate, and have low intra-observer, interobserver, and interscan variability rates.<sup>18</sup> The quantification of T2 offers a distinct advantage in the detection of global changes, in comparison with T2W imaging, which relies on regional differences in myocardial signal. There are 2 main types of T2 mapping techniques: spin-echo-based and T2-preparation (T2p) steady-state free-precession (SSFP)-based techniques, with the latter generally preferred. The underlying physics of the T2p-based technique is similar to that of the bright-blood T2-prepared SSFP sequence (see Part 1 of this review<sup>1</sup>).

Quantitative T2 methods have yielded promising results for the detection of myocardial involvement in patients with acute myocarditis and takotsubo cardiomyopathy. In these disease entities, T2 mapping showed more extensive myocardial involvement than was suggested by LGE, cine imaging, or T2W short tau inversion recovery (STIR) imaging.<sup>19</sup> It has been postulated that T2 mapping will enable accurate monitoring of the treatment and progression of disease.<sup>20</sup> In addition, T2 mapping techniques have been used to identify iron overload,<sup>21-23</sup> and quantitative T2 mapping has proved superior to both T2-STIR<sup>24</sup> and T2W imaging<sup>25</sup> for identification of myocardial edema in acute ischemic injury. However, these techniques have not been validated against a reliable histopathologic standard for the delineation of the area at risk. Moreover, the limited spatial resolution and the potential for misregistration between frames acquired with different T2 preparation times can lead to partial volume artifacts. Finally, high intersubject variability in myocardial T2 values has been reported in healthy volunteers,<sup>19,20</sup> which poses

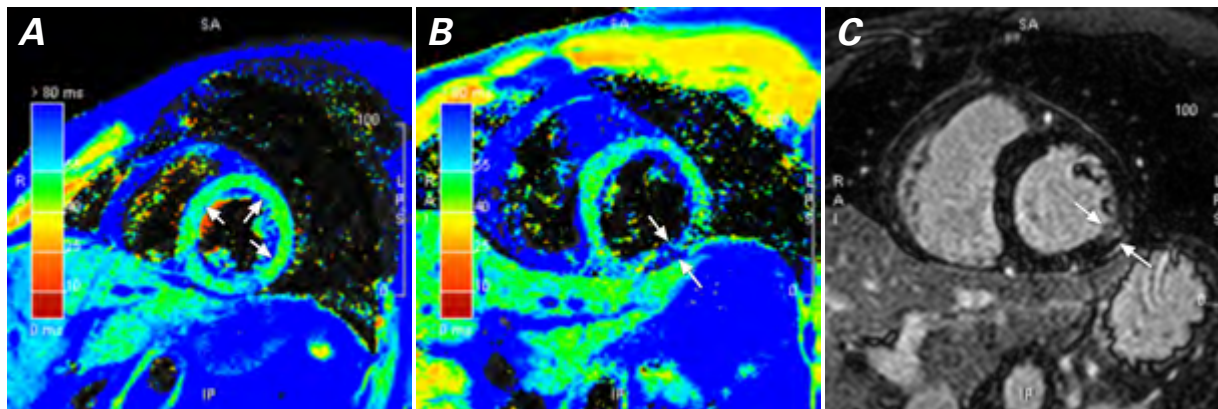


**Fig. 2** **A**) Parametric overlay of a T2 map on a short-axis slice of left ventricle (greenish ring) in a patient without myocardial abnormalities. The color scale of green in this image (arrows) corresponds to a normal mean T2 value of 45 ms. **B**) A 26-year-old man with myocarditis involving the inferolateral wall has normal T2 values throughout the septum and anterior wall but has abnormal T2 values with a mean of 71 ms in the inferolateral wall (arrows). **C**) The corresponding delayed-enhancement image shows enhancement in the same region of the inferolateral wall (arrows) in a pattern that is compatible with myocarditis.

significant challenges to the clinical application of T2 mapping, because the difference in T2 values between diseased and normal myocardium tends to be relatively small.<sup>26</sup>

### Free-Breathing Cine Techniques

Cine SSFP is the current workhorse sequence for ventricular function evaluation because of its superior blood-to-myocardium contrast and higher intrinsic SNR. One vital requirement for the SSFP sequence is uninterrupted radiofrequency (RF) excitation to maintain steady-state magnetization during suspended respiration. Therefore, a given scan-acquisition window is limited to the 10 to 20 seconds of breath-hold time. Similarly, because electrocardiographic (ECG) synchronization is crucial for data acquisition with SSFP sequences, routine cardiac cine SSFP sequences are acquired over multiple heartbeats—and MR data acquisition is synchronized to, or triggered by, the patient's recorded ECG signal. Volumetric coverage of the heart with use of SSFP involves the acquisition, over multiple breath-holds, of multiple individual 2-dimensional (2D) slices. This often increases the cumulative scan time. Moreover, this imaging technique might not be feasible in patients with impaired breath-holding capability, in sedated or noncooperative patients, or in pediatric patients. Also frequently encountered are erratic breathing patterns, irregular heart rates, large beat-to-beat variations in the R-R interval of the ECG (in patients with otherwise regular heart rates), and suboptimal ECG signal detection because of technical factors or patient factors (for example, distorted chest-wall geometry, pericardial effusion, or obesity). These variables often lead to motion artifacts, slice registration errors, and suboptimal image quality. Therefore, methods of image acquisition that do not require suspended respiration or ECG synchronization are highly desirable.

To this end, advances in hardware and postprocessing methods have facilitated the introduction and routine implementation of several new approaches. One approach, single-shot acquisition or real-time CMR, involves acquiring all of the required data for multiple images in a single heartbeat, without the need for ECG synchronization. However, this method typically results in inferior spatial and temporal resolution when compared with the resolution obtained with ECG-gated, segmented acquisition performed during suspended respiration. To overcome this limitation, real-time CMR is often combined with an image-acceleration technique called parallel imaging. Parallel imaging allows undersampling of MR data points—resulting in a reduction of SNR, although without a significant loss of diagnostic information. Parallel imaging can either accelerate the image-acquisition process to reduce the breath-hold time or improve the spatial or temporal resolution within a given imaging time.

A recently proposed fully automated image-acquisition method seeks to remedy the reduction in SNR.<sup>27,28</sup> With this method, the SNR of real-time CMR is retrospectively enhanced with respiratory motion-corrected averaging. This method has yielded image quality comparable to that achieved with the conventional method of image acquisition. In fact, the proposed technique provided superior image quality in patients with arrhythmia. A similar approach has also been validated for ECG-triggered, free-breathing DE-MR imaging during a single cardiac phase.<sup>29,30</sup> Another tactic is to use a respiratory-triggered, segmented SSFP sequence, which eliminates the breath-hold requirement in cine SSFP and has been validated in healthy volunteers and sedated children.<sup>31</sup> A recent study in adult patients showed that the LV functional values obtained with this respiratory-triggered free-breathing SSFP technique are in good agreement with the results obtained with a breath-hold SSFP sequence (Fig. 3).<sup>32</sup>

For triggering or gating purposes, self-gated techniques extract cardiorespiratory motion information directly from the acquired MR signals.<sup>33</sup> As a result, these techniques can be used without depending on breath-holding and ECG synchronization. Self-gating can be performed either retrospectively (after all data have been acquired) or prospectively (at the time of data acquisition). Retrospective techniques involve oversampling the MR data. These methods are not considered time efficient, because many data points have to be discarded at the time of data reconstruction.<sup>34</sup> Prospective techniques involve the real-time splitting of additionally acquired MR signal into data that represent cardiac and respiratory motion. In volunteers, 2D prospective cardiac-respiratory self-gating (CRSG) resulted in significantly decreased acquisition time with well-preserved image quality, compared with the retrospective technique.<sup>34</sup> Free-breathing 3-dimensional (3D) cine cardiac data are also being explored, because this technique offers the advantage of thin-slice, contiguous volume acquisition, which might augment the accuracy of measurements of functional values by eliminating slice misregistration errors. In one study, strong correlation was observed between LV and right ventricular functional values obtained with 3D prospective CRSG and those obtained with standard multislice 2D ECG-triggered, breath-hold imaging.<sup>33</sup> These developments are expected to reduce the complexity of CMR acquisition and to expand its application to a wider patient population.

### Coronary Magnetic Resonance Imaging

Coronary MR imaging, another evolving application of cardiac MR, is one of the most challenging of these applications. Some of the difficulties associated with this technique are inherent to noninvasive imaging of the coronary arteries. These include the small size, high tortuosity, and complex 3D anatomy of the coronary ar-



teries; their near-constant motion in accord with cardiac and respiratory cycles; and the surrounding signal from the adjacent epicardial fat and myocardium.<sup>35</sup> Other problems relate to the limited spatial and temporal resolution of the MR technology. Despite these challenges, several approaches for MR imaging of coronary arteries have been devised, in order to provide both high spatial resolution and high SNR. In the primary technique, the MR sequence is synchronized with the cardiac cycle (ECG-triggered), and data are acquired at the end-expiratory phase of respiration (respiratory-gated). In addition, preparatory RF pulses are used to suppress signal from the surrounding tissues, which improves the contrast-to-noise ratio of the coronary arteries. The 3D volumetric data set acquired is used to generate high-resolution and intuitive reconstructions of the coronary tree. As in computed tomographic coronary angiography, the image quality of coronary MR angiography (MRA) can be improved through pharmacologic control of the heart rate with  $\beta$ -blockers and dilation of the coronary arteries with nitroglycerin.<sup>36,37</sup> Technical advances such as higher-field-strength (3T) magnets, phased-array coils, parallel imaging techniques, and alternative methods of data acquisition such as spiral and radial MR imaging also enable faster acquisition, improved image quality, or both. Previously described free-breathing respiratory self-gated techniques are particularly useful for improving the efficiency and image quality of coronary MR imaging.<sup>38,39</sup>

One of the strengths of coronary MR imaging lies in its high accuracy in the detection of congenital anomalies of the origin and the proximal course of the coronary arteries (Fig. 4).<sup>40,41</sup> Coronary MR imaging is superior to invasive coronary angiography for delineating the course of anomalous vessels.<sup>42-44</sup> Anecdotal reports suggest that coronary MR can be used as part of a multisequence MR protocol to evaluate the functional and clinical significance of coronary artery anomalies.<sup>45,46</sup> Coronary MR imaging has also shown high accuracy in the identification and characterization of ectatic coronary vessels<sup>47</sup> and coronary artery aneurysms in children with Kawasaki disease.<sup>48-50</sup> However, the role of coronary MR imaging in coronary artery disease (CAD) is more limited. At present, coronary MR imaging can be used to identify CAD in the proximal half of the major coronary arteries, but it does not have the spatial resolution required to quantify and identify stenosis in the distal coronary arterial tree or in the side branches. Therefore, coronary MR imaging is currently used primarily to exclude a diagnosis of CAD in patients with suspected left main coronary artery or multivessel disease. Normal results on a coronary MR scan in this patient population have a high negative predictive value.<sup>44</sup> This technique can also be used in patients with a low likelihood of CAD, such as younger patients undergoing valvular surgery, and in patients with aor-

tic dissection or renal insufficiency for whom cardiac catheterization would be a high-risk procedure. In patients who present with LV systolic dysfunction in the absence of a history of MI, coronary MR imaging can be used to identify underlying multivessel CAD and to differentiate this condition from NICM.<sup>44</sup> Hence, coronary MR imaging remains a technically challenging application with narrow clinical usefulness that is currently being performed only at centers with considerable experience in cardiac MR.

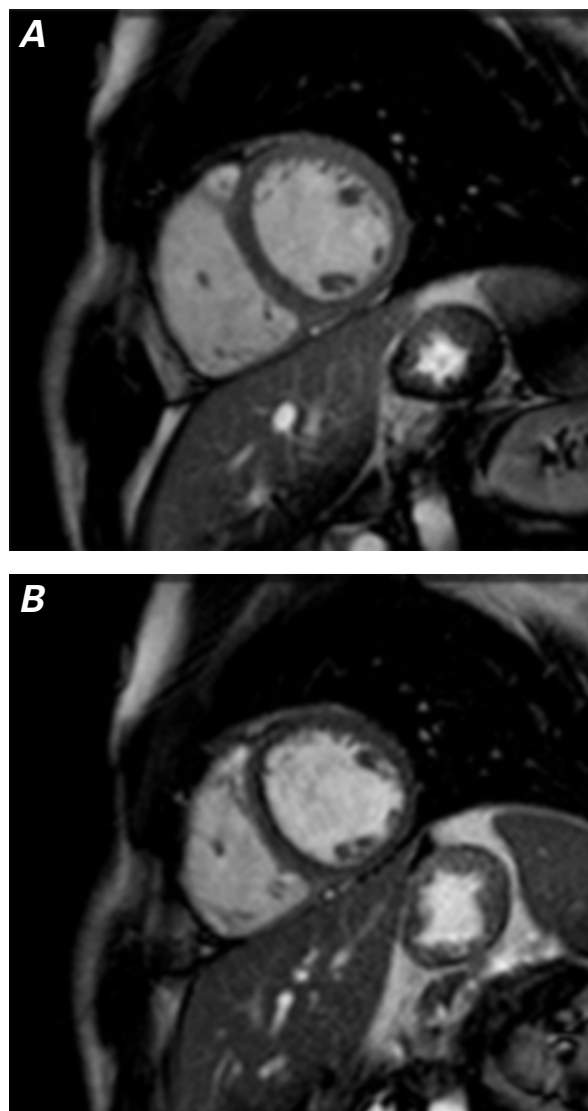


**Fig. 3** Short-axis cine steady-state free-precession dataset obtained **A**) with standard breath-hold technique and **B**) during free breathing in the same patient. Given the comparable contrast and the spatiotemporal resolution of the free-breathing technique, free breathing might be a viable alternative for the evaluation of left ventricular function in patients with impaired breath-holding capacity.

Supplemental motion images are available for Figures 3A and 3B.

## Heart Failure and Heart Transplantation

In a patient with newly diagnosed heart failure, CMR offers a clinically reliable toolbox for phenotypic characterization, identification of cause, and risk stratification for therapeutic management. Axial black-blood and SSFP images can characterize morphologic changes in the cardiac chambers, valves, and pericardium, and segmented cine SSFP images can help to evaluate the functional consequences of these morphologic changes. The combination of cine sequences and phase contrast (PC)-MR imaging provides a comprehensive overview of primary and secondary valvular dysfunctions that often coexist in patients with heart failure. The pattern of LGE on DE-MR imaging can then help to identify the origin of heart failure (Figs. 5 and 6). In fact, CMR has shown diagnostic accuracy superior or comparable

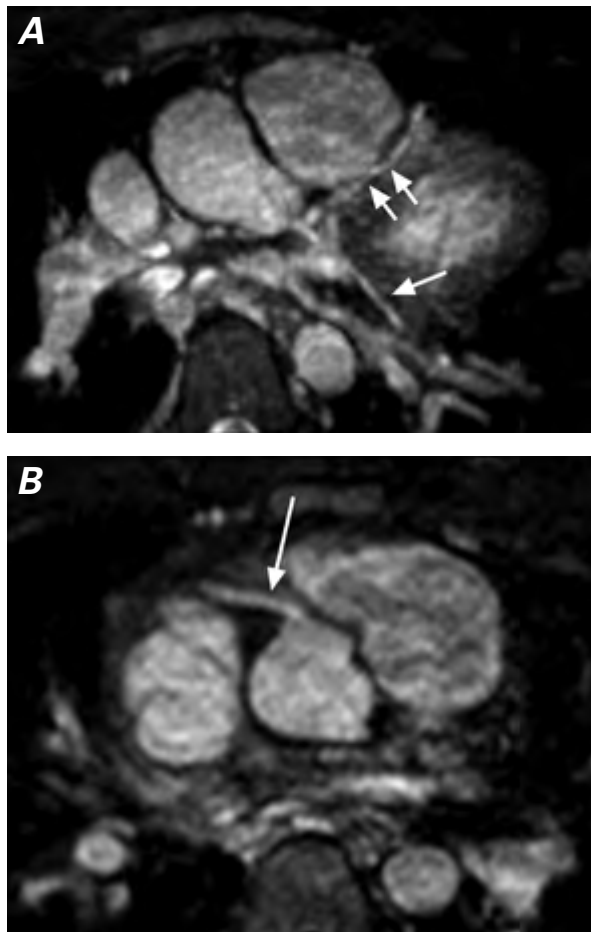


**Fig. 4** A 22-year-old man with a history of repaired tetralogy of Fallot underwent cardiac magnetic resonance imaging for evaluation and quantification of pulmonary insufficiency. Axial reformatted images from a navigator-gated, electrocardiogram-triggered, free-breathing, 3-dimensional steady-state free-precession volumetric dataset optimally show ostial and proximal courses of **A** the left anterior descending coronary artery (double arrows), the left circumflex coronary artery (single arrow), and **B** the right coronary artery (arrow).

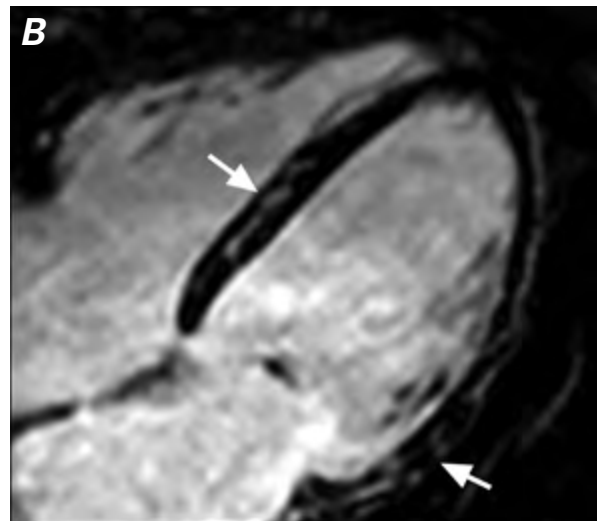
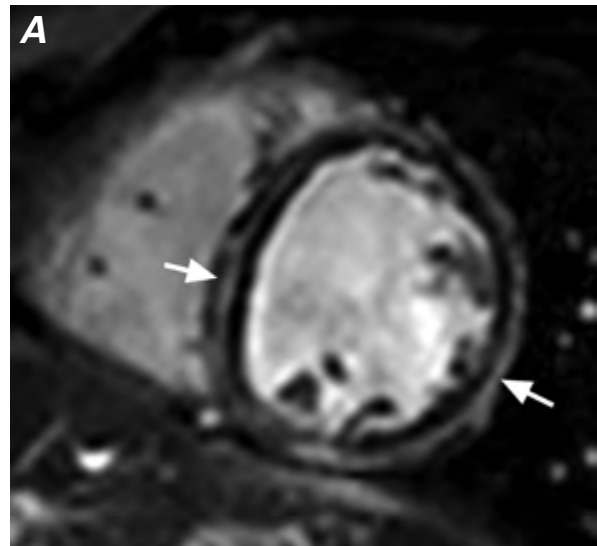


**Fig. 5** A 24-year-old woman with a history of epidermolysis bullosa and recent stroke underwent cardiac magnetic resonance imaging for evaluation of newly diagnosed systolic dysfunction on echocardiography. **A**) Short-axis and **B**) 4-chamber delayed-enhancement images show mild dilation of the left ventricle, moderate (predominantly mid-myocardial) enhancement in the septum, and predominantly epicardial enhancement in the anterior, lateral, and inferior walls (arrows). The noncoronary distribution and nonischemic pattern of delayed enhancement were consistent with myocarditis as the underlying cause of the patient's systolic dysfunction.

to that of endomyocardial biopsy (EMB) for the causal characterization of patients with heart failure.<sup>51</sup> Delayed enhancement-MR imaging is also superior to echocardiography in identifying such complications of heart failure as LV thrombus.<sup>52</sup> Perfusion imaging with use of dynamic contrast-enhanced (DCE)-MR can identify modifiable substrate, such as myocardial ischemia. Recently, CMR sequences such as myocardial tagging and PC-MRI have been used to identify and quantify mechanical dyssynchrony in patients with heart failure.<sup>53,54</sup>

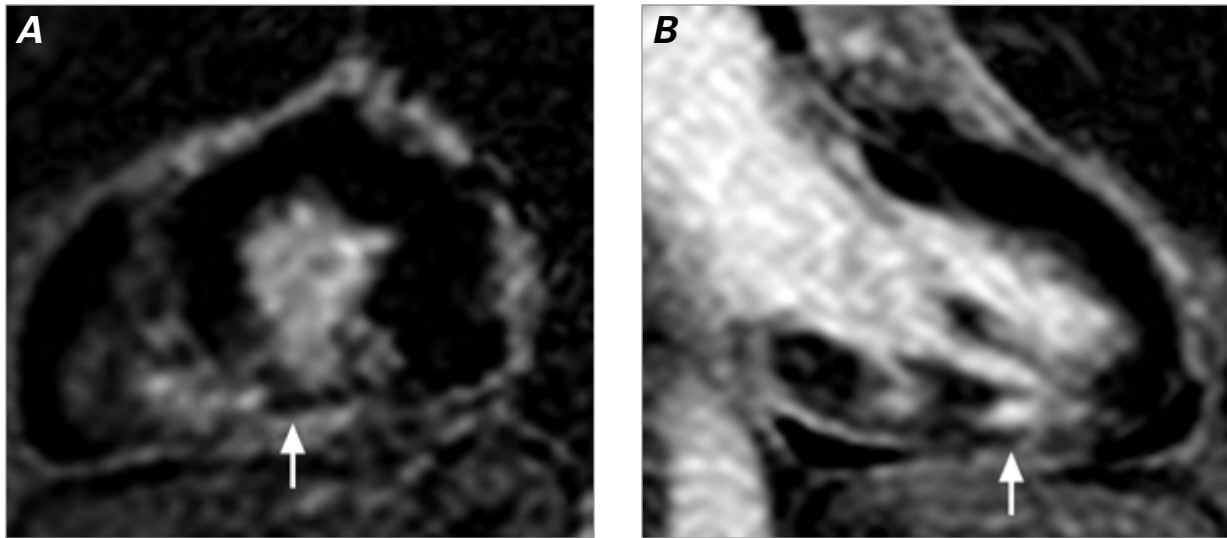


**Fig. 6** A 59-year-old woman with a history of left atrial myxoma resection presented with worsening heart failure shortly after that surgery. Right- and left-sided heart catheterization results were normal. Cine steady-state free-precession images (not shown) showed hypokinesia of the inferior wall. **A)** Short-axis and **B)** vertical long-axis delayed-enhancement images show subendocardial enhancement extending variably into the mid-myocardium (arrows) in the inferior wall in a coronary distribution (right coronary artery territory). The most likely cause of the patient's heart failure was an embolic phenomenon in the right coronary artery during the perioperative period, which resulted in ischemic insult.

Together with cardiac-function values and the pattern of LGE, these newer CMR acquisition and analysis techniques might better define the population of patients with heart failure who are most likely to benefit from cardiac resynchronization therapy (CRT). The extent of LGE on DE-MR imaging has also shown excellent accuracy for predicting clinical response to CRT.<sup>55</sup> As experience with MR-compatible implantation devices increases, CMR might come to play an increasingly important role in evaluating CRT benefits.

Cardiac MR is also being investigated as a potentially safer, noninvasive alternative to EMB for detecting acute cardiac allograft rejection (ACAR) in heart-transplant recipients. In a single-center study, T2 relaxation time (measured with a black-blood sequence) was found to be a sensitive marker of moderate ACAR. In that same study,<sup>56</sup> T2 relaxation time predicted the subsequent occurrence of such rejections in this patient population. Recently, quantitative T2 mapping was again shown to be a potential noninvasive tool for characterizing rejection in cardiac allografts.<sup>57</sup> A multisequence CMR protocol incorporating myocardial function, edema, and early and late postgadolinium enhancement has also shown high sensitivity and specificity for the detection of ACAR, compared with EMB.<sup>58</sup> Cardiac MR offers multiple potential advantages over EMB: it is noninvasive, is safe, and enables simultaneous myocardial tissue characterization and the evaluation of myocardial dysfunction resulting from allograft rejection. Given these attributes, CMR might provide guidance on the optimal timing and site of EMB in heart-transplant recipients. The usefulness of CMR in measuring response

to immunosuppressive therapy, conducting long-term follow-up of allografts, and detecting the sequelae of transplantation also merit further investigation.

### Conclusion

Cardiac MR is a versatile imaging technique that enables comprehensive noninvasive evaluation of cardiovascular physiology and disease. It has evolved from a focused research technique to a multifaceted clinical tool with wide and evolving applications. Although technically complex, CMR is highly accurate and cost-effective for the investigation, risk stratification, and evaluation of therapeutic response and prognosis in patients with cardiovascular diseases.

In this 2-part article, we have endeavored to distill the complex concepts of CMR to facilitate wider familiarity with and use of this robust technique. In addition, we have highlighted recent innovations and ongoing developments in CMR. Particular emphasis has been placed on those applications that appear to have the greatest potential for clinical integration in the near future. It is hoped that the information presented in these articles will enable referring physicians to better understand and integrate the power of CMR for improving patient outcomes and advancing the understanding of cardiovascular disorders.

### Acknowledgment

We are grateful for the editorial assistance of Megan M. Griffiths, scientific writer for the Imaging Institute, Cleveland Clinic, Cleveland, Ohio.

## References

1. Goenka AH, Flamm SD. Cardiac magnetic resonance imaging for the investigation of cardiovascular disorders. Part 1: current applications. *Tex Heart Inst J* 2014;41(1):7-20.
2. Piechnik SK, Ferreira VM, Dall'Armellina E, Cochlin LE, Greiser A, Neubauer S, Robson MD. Shortened Modified Look-Locker Inversion recovery (ShMOLLI) for clinical myocardial T1-mapping at 1.5 and 3 T within a 9 heartbeat breathhold. *J Cardiovasc Magn Reson* 2010;12:69.
3. Messroghli DR, Walters K, Plein S, Sparrow P, Friedrich MG, Ridgway JP, Sivananthan MU. Myocardial T1 mapping: application to patients with acute and chronic myocardial infarction. *Magn Reson Med* 2007;58(1):34-40.
4. Messroghli DR, Radjenovic A, Kozerke S, Higgins DM, Sivananthan MU, Ridgway JP. Modified Look-Locker inversion recovery (MOLLI) for high-resolution T1 mapping of the heart. *Magn Reson Med* 2004;52(1):141-6.
5. Goenka AH, Das CJ, Sharma R. Nephrogenic systemic fibrosis: a review of the new conundrum. *Natl Med J India* 2009; 22(6):302-6.
6. White SK, Sado DM, Flett AS, Moon JC. Characterising the myocardial interstitial space: the clinical relevance of non-invasive imaging. *Heart* 2012;98(10):773-9.
7. Moon JC, Messroghli DR, Kellman P, Piechnik SK, Robson MD, Ugander M, et al. Myocardial T1 mapping and extracellular volume quantification: a Society for Cardiovascular Magnetic Resonance (SCMR) and CMR Working Group of the European Society of Cardiology consensus statement. *J Cardiovasc Magn Reson* 2013;15:92.
8. Ferreira VM, Piechnik SK, Dall'Armellina E, Karamitsos TD, Francis JM, Choudhury RP, et al. Non-contrast T1-mapping detects acute myocardial edema with high diagnostic accuracy: a comparison to T2-weighted cardiovascular magnetic resonance. *J Cardiovasc Magn Reson* 2012;14:42.
9. Wong TC, Piehler K, Meier CG, Testa SM, Klock AM, Ancezi AA, et al. Association between extracellular matrix expansion quantified by cardiovascular magnetic resonance and short-term mortality. *Circulation* 2012;126(10):1206-16.
10. Wong TC, Piehler KM, Kang IA, Kadakkal A, Kellman P, Schwartzman DS, et al. Myocardial extracellular volume fraction quantified by cardiovascular magnetic resonance is increased in diabetes and associated with mortality and incident heart failure admission. *Eur Heart J* 2013 June 11 [Epub ahead of print]. doi: 10.1093/eurheartj/ehs193.
11. Flett AS, Hayward MP, Ashworth MT, Hansen MS, Taylor AM, Elliott PM, et al. Equilibrium contrast cardiovascular magnetic resonance for the measurement of diffuse myocardial fibrosis: preliminary validation in humans. *Circulation* 2010;122(2):138-44.
12. Puntmann VO, Voigt T, Chen Z, Mayr M, Karim R, Rhode K, et al. Native T1 mapping in differentiation of normal myocardium from diffuse disease in hypertrophic and dilated cardiomyopathy. *JACC Cardiovasc Imaging* 2013;6(4):475-84.
13. Sibley CT, Noureldin RA, Gai N, Nacif MS, Liu S, Turkbey EB, et al. T1 mapping in cardiomyopathy at cardiac MR: comparison with endomyocardial biopsy. *Radiology* 2012; 265(3):724-32.
14. Chan W, Duffy SJ, White DA, Gao XM, Du XJ, Ellims AH, et al. Acute left ventricular remodeling following myocardial infarction: coupling of regional healing with remote extracellular matrix expansion. *JACC Cardiovasc Imaging* 2012;5(9): 884-93.
15. Aletras AH, Tilak GS, Natanzon A, Hsu LY, Gonzalez FM, Hoyt RF Jr, Arai AE. Retrospective determination of the area at risk for reperfused acute myocardial infarction with T2-weighted cardiac magnetic resonance imaging: histopathological and displacement encoding with stimulated echoes (DENSE) functional validations. *Circulation* 2006;113(15): 1865-70.
16. Garcia-Dorado D, Oliveras J, Gili J, Sanz E, Perez-Villa F, Barrabes J, et al. Analysis of myocardial oedema by magnetic resonance imaging early after coronary artery occlusion with or without reperfusion [published erratum appears in *Cardiovasc Res* 1993;27(10):1889]. *Cardiovasc Res* 1993;27(8): 1462-9.
17. Arai AE, Leung S, Kellman P. Controversies in cardiovascular MR imaging: reasons why imaging myocardial T2 has clinical and pathophysiologic value in acute myocardial infarction. *Radiology* 2012;265(1):23-32.
18. Wassmuth R, Prothmann M, Utz W, Dieringer M, von Knobelsdorff-Brenkenhoff F, Greiser A, Schulz-Menger J. Variability and homogeneity of cardiovascular magnetic resonance myocardial T2-mapping in volunteers compared to patients with edema. *J Cardiovasc Magn Reson* 2013;15:27.
19. Thavendiranathan P, Walls M, Giri S, Verhaert D, Rajagopalan S, Moore S, et al. Improved detection of myocardial involvement in acute inflammatory cardiomyopathies using T2 mapping. *Circ Cardiovasc Imaging* 2012;5(1):102-10.
20. Giri S, Chung YC, Merchant A, Mihai G, Rajagopalan S, Raman SV, Simonetti OP. T2 quantification for improved detection of myocardial edema. *J Cardiovasc Magn Reson* 2009;11:56.
21. Guo H, Au WY, Cheung JS, Kim D, Jensen JH, Khong PL, et al. Myocardial T2 quantitation in patients with iron overload at 3 Tesla [published erratum appears in *J Magn Reson Imaging* 2009;30(5):1230]. *J Magn Reson Imaging* 2009;30(2): 394-400.
22. He T, Gatehouse PD, Anderson LJ, Tanner M, Keegan J, Pennell DJ, Firmin DN. Development of a novel optimized breathhold technique for myocardial T2 measurement in thalassemia. *J Magn Reson Imaging* 2006;24(3):580-5.
23. Kim D, Jensen JH, Wu EX, Sheth SS, Brittenham GM. Breathhold multiecho fast spin-echo pulse sequence for accurate R2 measurement in the heart and liver. *Magn Reson Med* 2009;62(2):300-6.
24. Verhaert D, Thavendiranathan P, Giri S, Mihai G, Rajagopalan S, Simonetti OP, Raman SV. Direct T2 quantification of myocardial edema in acute ischemic injury. *JACC Cardiovasc Imaging* 2011;4(3):269-78.
25. Park CH, Choi EY, Kwon HM, Hong BK, Lee BK, Yoon YW, et al. Quantitative T2 mapping for detecting myocardial edema after reperfusion of myocardial infarction: validation and comparison with T2-weighted images. *Int J Cardiovasc Imaging* 2013;29 Suppl 1:65-72.
26. von Knobelsdorff-Brenkenhoff F, Prothmann M, Dieringer MA, Wassmuth R, Greiser A, Schwenke C, et al. Myocardial T1 and T2 mapping at 3 T: reference values, influencing factors and implications. *J Cardiovasc Magn Reson* 2013;15(1): 53.
27. Kellman P, Chefd'hotel C, Lorenz CH, Mancini C, Arai AE, McVeigh ER. Fully automatic, retrospective enhancement of real-time acquired cardiac cine MR images using image-based navigators and respiratory motion-corrected averaging. *Magn Reson Med* 2008;59(4):771-8.
28. Kellman P, Chefd'hotel C, Lorenz CH, Mancini C, Arai AE, McVeigh ER. High spatial and temporal resolution cardiac cine MRI from retrospective reconstruction of data acquired in real time using motion correction and resorting. *Magn Reson Med* 2009;62(6):1557-64.
29. Kellman P, Larson AC, Hsu LY, Chung YC, Simonetti OP, McVeigh ER, Arai AE. Motion-corrected free-breathing delayed enhancement imaging of myocardial infarction. *Magn Reson Med* 2005;53(1):194-200.



30. Ledesma-Carbayo MJ, Kellman P, Hsu LY, Arai AE, McVeigh ER. Motion corrected free-breathing delayed-enhancement imaging of myocardial infarction using nonrigid registration. *J Magn Reson Imaging* 2007;26(1):184-90.
31. Krishnamurthy R, Pednekar A, Vogelius E, Atweh LA, Chu ZD, Zhang W, et al. Clinical validation of free breathing Respiratory Triggered Retrospectively Cardiac Gated Cine Steady-State Free Precession (RT-SSFP) imaging in sedated children [abstract]. *J Cardiovasc Magn Reson* 2013;15(suppl 1):O98. Available from: <http://www.jcmr-online.com/content/15/S1/O98> [cited 2014 Feb 20].
32. Wang H, Pednekar A, Goenka AH, Wuttichaipradit C, Berry S, Muthupillai R, Flamm S. Comparison of breath hold and free breathing respiratory triggered retrospectively cardiac gated cine steady-state free precession (RT-SSFP) imaging in adults [abstract]. *J Cardiovasc Magn Reson* 2014;16(suppl 1):P30. Available from: <http://www.jcmr-online.com/content/16/S1/P30> [cited 2014 Feb 20].
33. Manka R, Buehrer M, Boesiger P, Fleck E, Kozerke S. Performance of simultaneous cardiac-respiratory self-gated three-dimensional MR imaging of the heart: initial experience. *Radiology* 2010;255(3):909-16.
34. Buehrer M, Curcic J, Boesiger P, Kozerke S. Prospective self-gating for simultaneous compensation of cardiac and respiratory motion. *Magn Reson Med* 2008;60(3):683-90.
35. Manning WJ, Nezafat R, Appelbaum E, Danias PG, Hauser TH, Yeon SB. Coronary magnetic resonance imaging. *Magn Reson Imaging Clin N Am* 2007;15(4):609-37, vii.
36. Terashima M, Meyer CH, Keeffe BG, Putz EJ, de la Pena-Almaguer E, Yang PC, et al. Noninvasive assessment of coronary vasodilation using magnetic resonance angiography. *J Am Coll Cardiol* 2005;45(1):104-10.
37. Jin H, Zeng MS, Ge MY, Ma JY, Chen CZ, Shen JZ, Li RC. Influence of applying nitroglycerin in whole-heart free-breathing 3D coronary MR angiography. *AJR Am J Roentgenol* 2010;194(4):927-32.
38. Stehning C, Bornert P, Nehrke K, Eggers H, Stuber M. Free-breathing whole-heart coronary MRA with 3D radial SSFP and self-navigated image reconstruction. *Magn Reson Med* 2005;54(2):476-80.
39. Lai P, Larson AC, Bi X, Jerecic R, Li D. A dual-projection respiratory self-gating technique for whole-heart coronary MRA. *J Magn Reson Imaging* 2008;28(3):612-20.
40. Bunce NH, Lorenz CH, Keegan J, Lesser J, Reyes EM, Firmin DN, Pennell DJ. Coronary artery anomalies: assessment with free-breathing three-dimensional coronary MR angiography. *Radiology* 2003;227(1):201-8.
41. Rajiah P, Setser RM, Desai MY, Flamm SD, Arruda JL. Utility of free-breathing, whole-heart, three-dimensional magnetic resonance imaging in the assessment of coronary anatomy for congenital heart disease. *Pediatr Cardiol* 2011;32(4):418-25.
42. Taylor AM, Thorne SA, Rubens MB, Jhooti P, Keegan J, Gatehouse PD, et al. Coronary artery imaging in grown up congenital heart disease: complementary role of magnetic resonance and x-ray coronary angiography. *Circulation* 2000;101(14):1670-8.
43. McConnell MV, Ganz P, Selwyn AP, Li W, Edelman RR, Manning WJ. Identification of anomalous coronary arteries and their anatomic course by magnetic resonance coronary angiography. *Circulation* 1995;92(11):3158-62.
44. Kim WY, Danias PG, Stuber M, Flamm SD, Plein S, Nagel E, et al. Coronary magnetic resonance angiography for the detection of coronary stenoses. *N Engl J Med* 2001;345(26):1863-9.
45. Bunce NH, Rahman SL, Keegan J, Gatehouse PD, Lorenz CH, Pennell DJ. Anomalous coronary arteries: anatomic and functional assessment by coronary and perfusion cardiovascular magnetic resonance in three sisters. *J Cardiovasc Magn Reson* 2001;3(4):361-9.
46. Giorgi B, Dymarkowski S, Rademakers FE, Lebrun F, Bogaert J. Single coronary artery as cause of acute myocardial infarction in a 12-year-old girl: a comprehensive approach with MR imaging. *AJR Am J Roentgenol* 2002;179(6):1535-7.
47. Mavrogeni SI, Manginas A, Papadakis E, Foussas S, Douskou M, Baras P, et al. Correlation between magnetic resonance angiography (MRA) and quantitative coronary angiography (QCA) in ectatic coronary vessels. *J Cardiovasc Magn Reson* 2004;6(1):17-23.
48. Greil GF, Stuber M, Botnar RM, Kissinger KV, Geva T, Newburger JW, et al. Coronary magnetic resonance angiography in adolescents and young adults with Kawasaki disease. *Circulation* 2002;105(8):908-11.
49. Mavrogeni S, Papadopoulos G, Douskou M, Kaklis S, Seimenis I, Baras P, et al. Magnetic resonance angiography is equivalent to x-ray coronary angiography for the evaluation of coronary arteries in Kawasaki disease. *J Am Coll Cardiol* 2004;43(4):649-52.
50. Mavrogeni S, Papadopoulos G, Douskou M, Kaklis S, Seimenis I, Varlamis G, et al. Magnetic resonance angiography, function and viability evaluation in patients with Kawasaki disease. *J Cardiovasc Magn Reson* 2006;8(3):493-8.
51. Yoshida A, Ishibashi-Ueda H, Yamada N, Kanzaki H, Hasegawa T, Takahama H, et al. Direct comparison of the diagnostic capability of cardiac magnetic resonance and endomyocardial biopsy in patients with heart failure. *Eur J Heart Fail* 2013;15(2):166-75.
52. Mollet NR, Dymarkowski S, Volders W, Wathiong J, Herbots L, Rademakers FE, Bogaert J. Visualization of ventricular thrombi with contrast-enhanced magnetic resonance imaging in patients with ischemic heart disease. *Circulation* 2002;106(23):2873-6.
53. Lardo AC, Abraham TP, Kass DA. Magnetic resonance imaging assessment of ventricular dyssynchrony: current and emerging concepts. *J Am Coll Cardiol* 2005;46(12):2223-8.
54. Westenberg JJ, Lamb HJ, van der Geest RJ, Bleeker GB, Holman ER, Schalij MJ, et al. Assessment of left ventricular dyssynchrony in patients with conduction delay and idiopathic dilated cardiomyopathy: head-to-head comparison between tissue Doppler imaging and velocity-encoded magnetic resonance imaging. *J Am Coll Cardiol* 2006;47(10):2042-8.
55. White JA, Yee R, Yuan X, Krahn A, Skanes A, Parker M, et al. Delayed enhancement magnetic resonance imaging predicts response to cardiac resynchronization therapy in patients with intraventricular dyssynchrony. *J Am Coll Cardiol* 2006;48(10):1953-60.
56. Marie PY, Angioi M, Carreaux JP, Escanye JM, Mattei S, Tzvetanov K, et al. Detection and prediction of acute heart transplant rejection with the myocardial T2 determination provided by a black-blood magnetic resonance imaging sequence. *J Am Coll Cardiol* 2001;37(3):825-31.
57. Usman AA, Taimen K, Wasielewski M, McDonald J, Shah S, Giri S, et al. Cardiac magnetic resonance T2 mapping in the monitoring and follow-up of acute cardiac transplant rejection: a pilot study. *Circ Cardiovasc Imaging* 2012;5(6):782-90.
58. Taylor AJ, Vaddadi G, Pfluger H, Butler M, Bergin P, Leet A, et al. Diagnostic performance of multisequential cardiac magnetic resonance imaging in acute cardiac allograft rejection. *Eur J Heart Fail* 2010;12(1):45-51.